Dependance of Transition Metal Telluride Phases on Metal Precursor Reactivity and Mechanistic Implications

Danielle N. Penk*, Emma J. Endres*, Ahmed Y. Nuriye❄, Janet E. Macdonald*,†,⸸
*Department of Chemistry, †Vanderbilt Institute for Nanoscale Science and Engineering, Vanderbilt University, Nashville, Tennessee 37235, United States, and
❄Department of Chemistry, The Pennsylvania State University, Abington, PA 19001

Abstract

Modern bottom-up synthesis to nanocrystalline solid-state materials often lacks the reasoned product control that molecular chemistry boasts from having over a century of research and development. In this study, six transition metals including iron, cobalt, nickel, ruthenium, palladium, and platinum were reacted with the mild reagent didodecyl ditelluride in their acetylacetonate, chloride, bromide, iodide, and triflate salts. This systematic analysis demonstrates how rationally matching the reactivity of metal salts to the telluride precursor is necessary for the successful production of metal tellurides. The trends in reactivity suggest that radical stability is the better predictor of metal salt reactivity than hard–soft acid-base theory. Of the six transition metal tellurides, the first colloidal syntheses of iron and ruthenium tellurides ($FeTe_2$ and $RuTe_2$) are reported.

Introduction

The techniques used for the bottom-up synthesis of metal sulfides and selenides do not easily translate to the metal tellurides. Because of the soft nature of tellurium and more negative reduction potentials compared to that of sulfur and selenium ($E°_{Te, Te2-}$ = -1.143 V°, $E°_{Se, Se2-}$ = -0.924 V°, $E°_{S, S2-}$ = -0.476 V° vs SHE),[1] successfully capturing metal tellurides in the high temperature conditions common to nanocrystal synthesis can be challenging. Yet metal tellurides are important materials from an application standpoint. Iron,[2,3] cobalt,[4,5] and nickel[6,7] chalcogenides have a variety of applications as mercury capture materials, superconductors, catalysts, and as electromagnetic wave absorption materials. Additionally, ruthenium,[8,9] palladium,[10,11] and platinum,[12,13] chalcogenides have uses as catalysts, electrocatalysis, and suppressors of magnetoresistance. Metal sulfides and selenides have had more synthetic development than the telluride counterparts in bottom-up synthesis, leaving an area of underexplored potential and applications for these nanomaterials. We seek ways to rationally choose conditions that will be successful in the bottom up-syntheses to metal tellurides, rather than simply attempting (and often failing) the translation of conditions from the preparations of metals sulfides and selenides.

The metal tellurides chosen for this study have a wide variety of functions. For example, among the chosen first-row transition metals, iron tellurides have attracted attention for their applications in batteries and electrochemical sensors.[14,15] $FeTe_2$ nanoparticles were used as electrochemical sensors to detect dopamine, uric acid, guanine and adenine simultaneously to facilitate early detection of a variety of diseases including Parkinson's disease, schizophrenia, and AIDS.[15] Cobalt tellurides are active electrocatalysts and photocatalysts,[16,17,18] including the use of CoTe nanoparticles, which serve as photocatalysts for the reduction of carbon dioxide into methane.[18] Additionally, researchers have shown an interest in nickel tellurides for their applications in electrocatalysis, electronics, and optoelectronics.[19,20,21] $NiTe_2$ nanoparticles were studied for their potential use as electrocatalysts for hydrogen evolution.[21] Among the second and third-row transition metals, palladium tellurides are of considerable interest for their catalytic properties.[22,23] For instance, PdTe and Pd_9Te_4 have been tested as catalysts in a classic organic reaction, the Suzuki-Miyaura coupling.[23,24] In contrast to the transition metal tellurides discussed so far, platinum tellurides remain elusive amidst the literature; however, they have intriguing plasmonic and electrocatalytic properties.[25,26,27] Similarly, very little is known about the characteristic properties of ruthenium tellurides. The ruthenium tellurides are a particularly underexplored space, but other ruthenium chalcogenides are powerful hydrodesulfurization catalysis and supercapacitor materials.[28,29] However, from what *is* known, $RuTe_2$ can perform hydrogen evolution and has semiconducting abilities.[30,31] Phase diagrams have been reported for iron, cobalt, nickel, ruthenium, palladium, and platinum tellurides;[32,33] however, very few colloidal syntheses have been reported for any of the known phases.

In aqueous conditions, dissolved tellurite and tellurate anions can be employed as tellurium sources. Yuan *et al.* synthesized FeTe from mixtures of Te nanorods and $FeCl_3 \cdot 6H_2O$,[34] where hydrazine was used to reduce dissolved TeO_2 to form the Te nanorod precursors. Praminik and coworkers dissolved TeO_2 in highly basic solution, and then used $NaBH_4$ as a reducing agent in the presence of various metal salts. The authors chose this route to make CoTe, NiTe,[35] and $FeTe_2$.[15] In contrast, Masikini *et al.* dissolved $PdCl_2$ in a highly basic solution of NaOH and used H_2Te gas to form PdTe quantum dots.[36] Lastly, Feng and coworkers used $NaTeO_3$ and $RuCl_3$ to prepare $RuTe_2$ supported on graphene.[30]

In addition to aqueous conditions, solid-state synthesis is commonly used to make transition metal tellurides. Campos *et al.* utilized ball milling to access the iron-rich phase of Fe_5Te_4.[37] Furthermore, the Pumera group accessed $CoTe_2$ and $NiTe_2$ by heating their corresponding stoichiometric ratios of cobalt, nickel and tellurium powders to 1000 °C.[21] Li and coworkers synthesized NiTe from nickel bis(dimethylglyoxime) and Te powder at temperatures of 700 and 800 °C for four hours.[38] In a similar fashion, Gusmão *et al.* heated the appropriate amounts of platinum and tellurium powders to 950 °C for 10 days to synthesize $PtTe_2$ and Pt_3Te_4.[26] Finally, Tsay *et al.* synthesized $RuTe_2$ by heating elemental ruthenium and tellurium powders in a quartz ampoule to 1000 °C for 10 days.[31]

Other varieties of synthesis have been performed to access metal tellurides as well. Kang and coworkers synthesized yolk-shell structured FeTe@C and $FeTe_2$@$FeTe_2$-C nanospheres by reductively tellurizing iron nitrate-C nanospheres with H_2Te gas at 400 or 700 °C.[14] $NiTe_2$ was prepared in a similar fashion by Duan *et al.*, where $NiCl_2$ was reductively tellurized with H_2Te gas from 550-700 °C.[20] In contrast, Fu and coworkers synthesized $PtTe_2$ crystals through van der Waals epitaxial growth on mica.[25] The authors chose a salts-assisted evaporation strategy to form a homogeneous $PtCl_4$/NaCl precursor. Both the precursor and tellurium powder were placed in a quartz tube and heated to 800 ºC for 30 min under 10% H_2/Ar gas to produce $PtTe_2$ crystals.

For the noble metals of Pd and Pt, preparations become tricky because of their propensity to simply form metal(0) particles. Single source precursors are a way to ensure bonding between the metal and tellurium. Singh *et al.* synthesized PdTe nanoparticles from single source precursors decorated with organic frameworks.[22] Similarly, Kumar and coworkers synthesized PdTe and Pd_9Te_4 nanoparticles through thermolysis of Pd^{2+} complexes.[23] Lastly, Afzaal and coworkers synthesized a variety of transition metal tellurides, including $FeTe_2$, NiTe, PdTe, PtTe and $PtTe_2$ from ditelluroimidodiphosphinate complexes.[27]

Still other research groups prefer other synthetic methods to access metal tellurides. Shrestha *et al*. synthesized CoTe thin films through the anion exchange of cobalt hydroxycarbonate with an aqueous tellurium powder solution.[17] Ashiq *et al.* utilized hydrazine as the reducing agent for Te(0) in a hydrothermal approach to synthesize CoTe.[18] Nath *et al*. used a similar hydrothermal reaction except with TeO_2 to give Ni_3Te_2. Alternatively, the same group synthesized Ni_3Te_2 films through reductive electrodeposition from a solution of $NiSO_4 \cdot 6H_2O$ and

TeO_2 onto Au coated glass slides.[19] Lastly, Xie *et al*. used a solvothermal approach with $CoCl_2 \cdot 6H_2O$ and Te(0) powder at 160 °C to synthesize $CoTe_2$ nanorods.[39]

To summarize, the transition metal tellurides of iron, cobalt, nickel, ruthenium, palladium, and platinum have a variety of applications that demand further study. The common methods to synthesize these transition metal tellurides mentioned thus far include aqueous conditions, solid-state methods, epitaxial growth, single-source precursors, anion exchange, reductive electrodeposition, and solvothermal approaches in autoclaves. As the aforementioned syntheses demonstrate, the methods for synthesizing transition metal tellurides often involve high temperatures, long reaction times, and specialized equipment. There are only a few examples in the literature where colloidal synthesis is utilized, in part, because there are only three common tellurium reagents that have been employed.

The Schaak group used *bis*(trimethylsilyl)telluride or TOP-Te to tellurize metal(0) particles to prepare a plethora of transition metal tellurides including: $CoTe_2$, $NiTe_2$, PdTe, $PdTe_2$, $PtTe_2$, Ag_2Te, and $RhTe_2$.[40] In the presence of *bis*(trimethylsilyl)telluride, a more-reactive tellurium reagent, generally, the more tellurium rich phases like $PdTe_2$ are obtained. Unfortunately, one disadvantage to *bis*(trimethylsilyl)telluride is that it is volatile and very toxic. The less reactive tellurium reagent, TOP-Te, produced the less tellurium rich phase of PdTe. By altering the tellurium reagent's reactivity, they were able to obtain phase control of PdTe *vs* $PdTe_2$. In another solution phase synthesis, Yu and coworkers selectively prepared CoTe or $CoTe_2$ nanofleeces by reacting Te nanowires with $Co(acac)_2$ at 200 °C.[16] Phase control was obtained by altering the millimoles of the cobalt precursor present.

In contrast to the bottom-up preparations, solid-state procedures using stoichiometric mixtures of the metals and tellurium have long produced a larger variety of phases including: Fe_5Te_4, $CoTe_2$, NiTe, $NiTe_2$, Pt_3Te_4, $PtTe_2$, and $RuTe_2$. Among these phases only $CoTe_2$, $NiTe_2$, and $PtTe_2$ have been accessed *via* colloidal synthesis. Because of this gap of missing phases in the literature from colloidal synthesis, more work must be done to investigate how to obtain the more exotic phases, typically only observed under solid-state reaction conditions.

Our group has pioneered the use of didodecyl ditelluride as an exceedingly mild reagent for the synthesis of copper tellurides, as it reacts at temperatures that are considered low for colloidal synthesis (< 200 °C). For

example, we obtained a metastable phase of $Cu_{1.5}Te$ and CuTe at 135 °C and 155 °C, respectively.[41] An added benefit of didodecyl ditelluride is that the red solid has minimal stench, unlike the corresponding selenide. Other than limiting extended light exposure and storage at 0 °C, no special training is required to use or handle this chemical. With the scalability of colloidal synthesis and the mild reaction conditions particularly afforded by this new reagent, didodecyl ditelluride, there is potential to readily prepare kinetically trapped phases to allow for a more extensive study and use of metal tellurides in applications. However, as a very mild reagent, it is likely that the limiting component will not be the reactivity of the telluride reagent, but rather that of the metal source. Both must be reactive enough at moderate temperatures to reap the rewards of the mild tellurium source.

Thus, how does one choose a metal source? Toxicity and safety can be a concern, and an infamous example is the early cadmium chalcogenide quantum dot synthesis which used a toxic $CdMe_2$ reagent, but now CdO is almost exclusively used.[42] Solubility in heavy organic media is a consideration, and long chain-ligands, such as carboxylates and amines, have been employed either intentionally or serendipitously. For example, recognizing that cadmium oleate binds as a Z-type ligand is important to consider.[43,44] The counterions from the metal source were also long under examination in their role in surface passivation of the growing crystals.[45] To our knowledge, there has not been a systematic study of how the inherent reactivity of the metal precursor can influence the product phase in bottom-up synthesis.

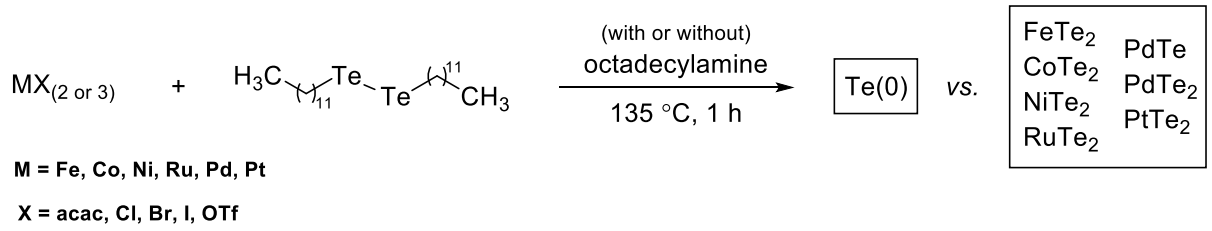

Scheme 1. The reaction of various metal precursors with didodecyl ditelluride gives Tellurium or Transition Metal Tellurides.

Herein, this work describes a solution phase synthesis of iron, cobalt, nickel, ruthenium, palladium, and platinum tellurides under mild reaction temperatures and times using metal acetylacetonate, chloride, bromide, iodide, and triflate salts and didodecyl ditelluride (**Scheme 1**). It was found that modulating the reactivity of the chosen transition metal precursor determined whether a metal telluride was achieved and, in the particular case of the palladium tellurides, determined the phase. The results suggest the trends in reactivity are correlated with

radical stability of the metal precursor. Of these six transition metal tellurides, the first nanoparticle syntheses of iron and ruthenium tellurides *via* colloidal syntheses are reported.

Experimental Section

Materials

All reactions were performed in oven-dried 15 mL three neck round-bottomed flasks using standard Schlenk line techniques under an argon atmosphere. Reaction temperatures were controlled using a thermocouple, and stirring rates were set to 1,200 rpm. Reactions without octadecylamine were degassed at 80 °C for 30 min prior to injection; reactions with octadecylamine and/or metal hydrates were degassed at (100 – 135) °C for 1 h to remove water prior to injection.

Cobalt(II) acetylacetonate ($Co(acac)_2$, 97%), cobalt(II) chloride anhydrous ($CoCl_2$, ≥98%), dioctyl ether (99%), iron(II) acetylacetonate ($Fe(acac)_2$, 99.95% trace metals basis), iron(II) bromide anhydrous ($FeBr_2$, 98%), iron(II) iodide anhydrobeads (FeI_2, ≥99.99% trace metals basis), nickel(II) acetylacetonate ($Ni(acac)_2$, 95%), nickel(II) chloride hexahydrate ($NiCl_2 \cdot 6H_2O$, 99.9%), octadecylamine (97%), and trifluoromethanesulfonic acid (≥99%) were obtained from Sigma Aldrich. Cobalt(II) bromide hydrate ($CoBr_2 \cdot XH_2O$), cobalt(II) iodide anhydrous (CoI_2, min. 95%), cobalt(II) trifluoromethanesulfonate ($Co(OTf)_2$, 98%), iron(II) chloride anhydrous ($FeCl_2$, 98%), iron(II) trifluoromethanesulfonate ($Fe(OTf)_2$, 98%), nickel(II) bromide ($NiBr_2$ anhydrous, 99+%), nickel(II) trifluoromethanesulfonate ($Ni(OTf)_2$, 98%), palladium(II) acetylacetonate ($Pd(acac)_2$, 99%), palladium(II) bromide ($PdBr_2$, 99%), palladium(II) chloride ($PdCl_2$, 99.9%), palladium(II) iodide (PdI_2, 99%), palladium(II) nitrate hydrate ($Pd(NO_3)_2 \cdot XH_2O$) (Pd ~40%, 99.9%-Pd), platinum(II) acetylacetonate ($Pt(acac)_2$, 98%), platinum(II) bromide ($PtBr_2$, 98%), platinum(II) chloride ($PtCl_2$, 99.9%), platinum(II) iodide (PtI_2, min. 98%), ruthenium(III) acetylacetonate ($Ru(acac)_3$, 99%), ruthenium(III) bromide hydrate ($RuBr_3 \cdot XH_2O$), ruthenium(III) chloride anhydrous ($RuCl_3$), and ruthenium(III) iodide anhydrous (RuI_3, 98+%) were obtained from Strem Chemicals. XRD analysis of the ruthenium(III) chloride found it to be instead $RuOCl_2$.[46] Nickel(II) iodide (NiI_2, 98%) was obtained from Ambeed, Inc. All materials were used from the commercial suppliers without further purification.

Synthesis of Transition Metal Telluride (No Ligand)

A solution of metal precursor (0.25 mmol) in dioctyl ether (2.5 mL) was placed in a 15 mL three-neck round bottom flask and was degassed under vacuum at 80 °C for 30 min. A solution of didodecyl ditelluride (0.25 mmol) in dioctyl ether (1.0 mL) was degassed under vacuum at room temperature for 30 min. Both flasks were placed under an argon atmosphere, and then evacuated and refilled with argon three times. The reaction flask containing the metal precursor was heated to 135 °C, and the telluride precursor was injected into the reaction vessel. The reaction mixture was allowed to stir for 1 h and then cool to room temperature. The post reaction mixture was precipitated in acetone, centrifuged (8000 rpm, 8 min) and resuspended in chloroform two to three times.

Synthesis of Transition Metal Telluride (with Octadecylamine)

A solution of metal precursor (0.25 mmol) and octadecylamine (0.50 mmol) in dioctyl ether (2.5 mL) was placed in a 15 mL three-neck round bottom flask and was degassed under vacuum at (100-135) °C for 1 h. A solution of didodecyl ditelluride (0.25 mmol) in dioctyl ether (1.0 mL) was degassed under vacuum at room temperature for 1 h. Both flasks were placed under an argon atmosphere, and then evacuated and refilled with argon three times. The reaction flask containing the metal precursor was heated to 135 °C, and the telluride precursor was injected into the reaction vessel. The reaction mixture was allowed to stir for 1 h and then cool to room temperature. The post reaction mixture was precipitated in warm isopropanol, centrifuged (8000 rpm, 8 min) and resuspended in chloroform two to three times.

Synthesis of Palladium Trifluoromethanesulfonate $Pd(OTf)_2$

To a solution of $Pd(NO_3)_2 \cdot XH_2O$ (57.9 mg, 0.25 mmol) in H_2O (8 drops) was added trifluoromethanesulfonic acid (0.88 mL, 10 mmol) dropwise at 0 °C. The resulting purple suspension was allowed to warm to room temperature and stir for 2 h. The post reaction mixture was precipitated with dioctyl ether (8000 rpm, 8 min). The crude material was immediately carried forward into the next reaction with didodecyl ditelluride. This procedure is adapted from the literature.[47]

Characterization

Transmission Electron Microscopy (TEM) was performed on a FEI Technai Osiris 200 kV S/TEM system with EDS mapping capabilities. TEM samples were prepared by dropping a $CHCl_3$ suspension of the nanoparticles onto a carbon coated Cu or Ni grid. X-ray Diffraction (XRD) measurements were performed using a Rigaku SmartLab powder X-ray diffractometer with a CuKα (λ = 0.154 nm) radiation source set to 40 kV and 44 mA, and a D/teX Ultra 250 1D silicon strip detector. XRD patterns were acquired using a step size of 0.1 ° at 2.5 °/min.

Results and Discussion

In previous works, our lab has established novel syntheses to copper chalcogenides using didodecyl diselenide and didodecyl ditelluride. These syntheses were notable in that the copper chalcogenide products were rare metastable phases such as wurtzite-like $Cu_{2-x}Se$[48] and $Cu_{1.5}Te$[41] as well as the first reported colloidal synthesis of vulcanite CuTe.[41] The reagents reacted at moderate temperatures for nanocrystal syntheses: didodecyl diselenide (155 °C) and didodecyl ditelluride (135 and 155 °C). The low synthetic temperatures may partially explain the ability of these reagents to trap the metastable phases and prevent transformations to more thermodynamically stable phases typically observed at higher reaction temperatures.

Control studies indicate that matching the reactivity of the telluride precursor to that of the metal source is important, since the tellurium precursor can decompose on its own at elevated temperatures; didodecyl ditelluride heated to 135 °C for 1 h yields tellurium metal. In the reported syntheses of $Cu_{1.5}Te$ and CuTe,[41] $Cu(acac)_2$ was employed as a copper source. It was reactive at the moderate synthetic temperatures of 135 and 155 °C and able to "capture" the Te precursor before decomposition. This result reinforced the hypothesis that in order to obtain a desired transition metal telluride, the intervention of a metal precursor with comparable reactivity would be needed to form a metal telluride and prevent the decomposition of the didodecyl ditelluride to Te(0).

Herein, we further the use of didodecyl ditelluride as a useful reagent for the synthesis of a broad range of metal tellurides. However, as one ventures farther from Cu on the periodic table, the bond strength and chemistry of the metal precursors will change the reaction landscape. Poor reactivity of the metal precursor may prevent the

formation of metal tellurides. Furthermore, when more than one phase of metal telluride is possible, the reactivity of the metal precursor may also influence the resultant phase. For this reason, a comprehensive and systematic study of a variety of metal precursors was performed to provide rational, predictable trends.

Transition metal tellurides of iron, cobalt, nickel, ruthenium, palladium, and platinum were synthesized from various metal precursors of acetylacetonates, chlorides, bromides, iodides, and triflates with didodecyl ditelluride. For consistency, a 1:1 molar ratio (i.e. 1 metal atom : 2 tellurium atoms) of the reagents were used in dioctyl ether at a constant reaction temperature of 135 °C for 1 h. XRD was used to identify the crystalline products (**Figures 1** & **2**), which are summarized in **Tables 1** & **2**. Metal tellurides were identified for all the metals studied including $FeTe_2$ (Frohbergite), $CoTe_2$ (Cobalt Telluride), $NiTe_2$ (Melonite), $RuTe_2$ (Ruthenium Telluride), PdTe (Kotulskite), $PdTe_2$ (Merenskyite) and $PtTe_2$ (Moncheite). Of particular note, these are the first reported colloidal syntheses of $FeTe_2$ and $RuTe_2$.

$FeTe_2$ and $RuTe_2$ have marcasite and pyrite structures, respectively, and were straight forward to identify by XRD. In contrast, $CoTe_2$, $NiTe_2$, $PdTe_2$ and $PtTe_2$ all have layered $Cd(OH)_2$ structures which sometimes can be challenging to distinguish from the MTe phases by XRD in nanomaterials. EDS was employed to confirm the MTe_2 stoichiometry (See Supporting Information); however, because the differentiation between NiTe *vs* $NiTe_2$ and PdTe *vs* $PdTe_2$ was very clear by XRD, EDS was not deemed necessary for these metal telluride materials.

It was found that there was a critical dependance of the reaction products on the choice of metal precursor (**Table 1** & **Figure 1**). Among the first-row transition metals (Fe, Co, and Ni), the acetylacetonates and chlorides only produced tellurium metal, which indicates these precursors were not reactive enough to produce metal

Table 1. Phases (no ligand)

Precursor	Fe	Co	Ni	Ru[a]	Pd	Pt
$M(acac)_2$	Te	Te	Te	Te	PdTe	$PtTe_2$
MCl_2	Te	Te	Te	Te, $RuOCl_2$	PdTe, $PdTe_2$	$PtTe_2$
MBr_2	Te	Te	$NiTe_2$	Ru	PdTe, $PdTe_2$	$PtTe_2$
MI_2	$FeTe_2$, Fe	$CoTe_2$	$NiTe_2$	$RuTe_2$	$PdTe_2$	$PtTe_2$
$M(OTf)_2$	Te	Te	Te	–	$PdTe_2$	–

[a]All ruthenium precursors utilized were in the +3 oxidation state. The purchased "$RuCl_3$" precursor was analyzed by XRD and found to be $RuOCl_2$. *vide infra*.

tellurides. While $NiBr_2$ did produce a telluride ($NiTe_2$), only the iodides for all three metals consistently provided a metal telluride product.

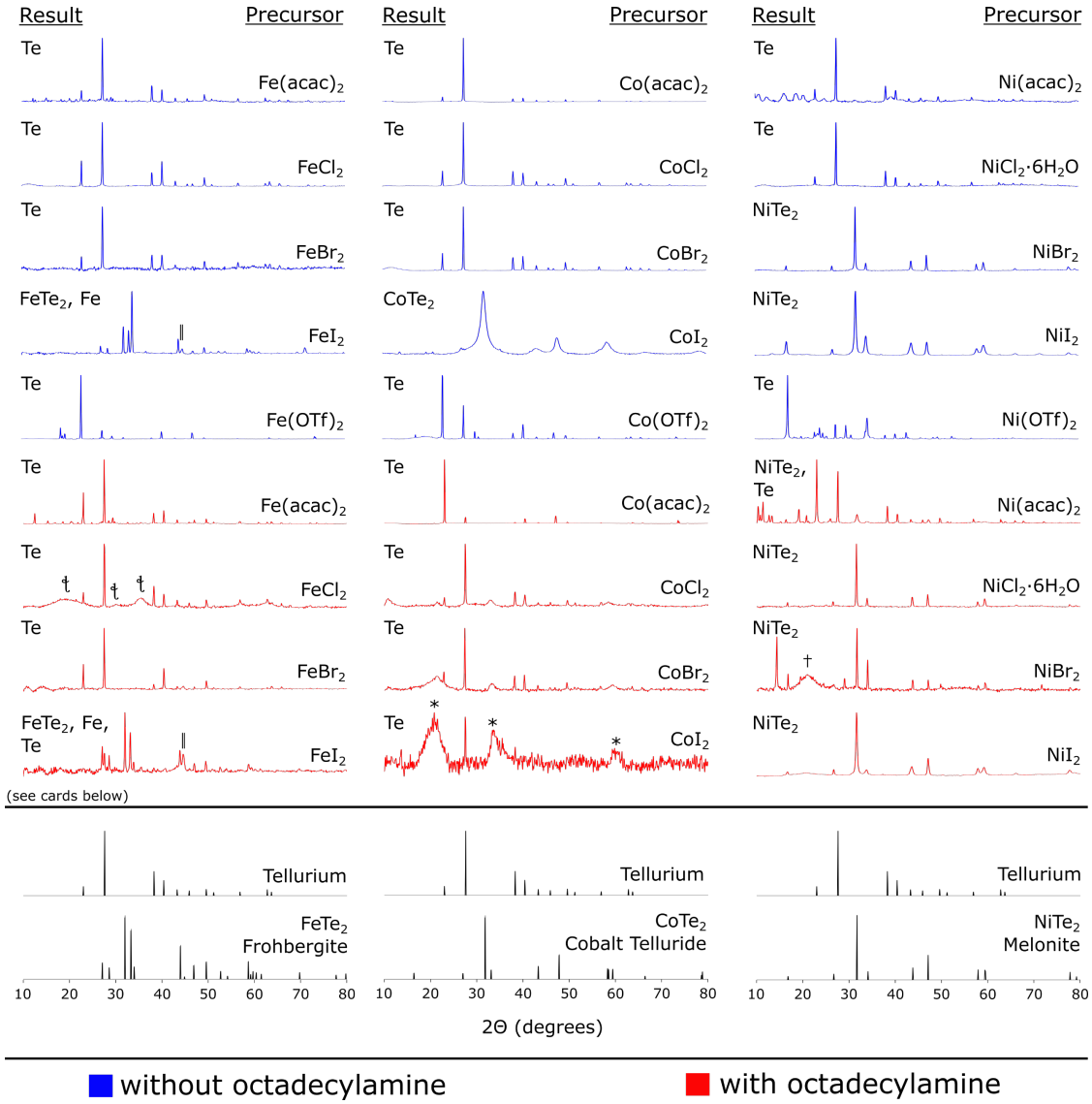

Figure 1. XRD of the products of iron, cobalt and nickel salts with didodecyl ditelluride. ICDD: ‖ Fe: #4113931. ϟ Magnetite: #159959. * Different polymorph of CoI_2 confirmed by EDS. † Amorphous octadecylamine (See ESI). Tellurium: #1011098, Frohbergite: #77319, Cobalt Telluride: #625401, Melonite: #159382. (For convenience starting metal precursors for every experiment were indicated above each corresponding XRD trace.)

The trend in reactivity of the first-row transition metal precursors appears to match hard–soft acid-base (HSAB) theory. $Fe(acac)_2$, $Co(acac)_2$, and $Ni(acac)_2$ as well as $FeCl_2$, $CoCl_2$, and $NiCl_2$ are the least reactive metal precursors due to the hard-hard interactions and strong-orbital-overlapping characteristics of these reagents. The inability to react with didodecyl ditelluride caused only decomposition to Te(0) to be observed. Contrastingly,

metal iodides were expected to be most reactive due to the hard-soft interactions and poor orbital overlap. Indeed, these were the reagents that gave tellurium-rich phases of $FeTe_2$, $CoTe_2$ and $NiTe_2$. ($FeTe_2$ was particularly prone to oxidation; air-free purification and characterization were needed.) The lattice energies (*U)* of the halide salts illustrate the trend in bond strength where the stability follows $MCl_2 > MBr_2 > MI_2$ for first-row transition metals ($U_{FeCl2} - U_{FeI2}$ = 130 kJ/mol, $U_{CoCl2} - U_{CoI2}$ = 138 kJ/mol, $U_{NiCl2} - U_{NiI2}$ = 146 kJ/mol).[49] However, lattice energies cannot explain why of the bromides, $NiBr_2$ was the only one to provide a metal telluride; $NiBr_2$ is actually the most stable of the three bromides by an amount even greater than the changes through the halides (U_{FeBr2} - U_{NiBr2} = -214 kJ/mol). Similarly, HSAB did not explain the results of the second and third-row metals (*vide infra*).

An alternative hypothesis proposes that the reactivity correlates with the stability of a radical halide, which follows $Cl^{\bullet} < Br^{\bullet} < I^{\bullet}$.[50] In general, halides can undergo *both* one and two-electron chemistry. A good demonstration of this phenomenon is the Finkelstein reaction in which the S_N2 displacement of a primary alkyl halide is replaced with another halide in a two-electron fashion. However, there are reported instances of sequential cation-free radical mechanisms where dimeric and rearranged products can occur.[51,52]

To test if one or two-electron chemistry dominates the reactivity of these systems, the products resulting from metal halide and triflate precursors were compared. It is known that metal halides and triflates often have comparable chemistry, but what distinguished the triflates is that they do not easily undergo one-electron chemistry, unlike halides. Triflates are known to be excellent leaving groups in two-electron chemistry such as S_N1 and S_N2 reactions, which follows $Cl^- < Br^- < I^- < OTf^-$.[53] Metal triflates similarly are considered "super Lewis Acids".[54] Thus, a comparison of the reactivity of metal halides with metal triflates can provide evidence for one or two-electron chemistry.

The first-row transition metal triflates of iron, cobalt, and nickel each reacted with didodecyl ditelluride at 135 °C for 1 h to compare to the metal halides. $Fe(OTf)_2$, $Co(OTf)_2$, and $Ni(OTf)_2$ were all unreactive with the didodecyl ditelluride, and instead only Te metal and polymorphs of the triflate precursors were isolated (identified through control reactions without the presence of didodecyl ditelluride (**Table 1** & **Figure 1**, See Supporting Information). Since the triflates were unreactive towards the didodecyl ditelluride, yet the iron, cobalt and nickel(II) iodides and nickel(II) bromide were, they must undergo a differing reaction mechanism. It can be

cautiously hypothesized that one-electron chemistry dominates this reaction of metal halides with didodecyl ditelluride to form metal tellurides.

The second and third-row metals (Ru, Pd, and Pt) appear to undergo more complex chemistry which further indicates that HSAB theory does not adequately explain the observed phases (**Table 1** & **Figure 2**). Among the palladium series, all reagents were reactive enough to provide a metal telluride phase. The lattice energies have not been reported for Ru and Pt salts, however, they are available for Pd. The difference in energy across the halides is less than a quarter of that for the first-row metals of Fe Co, and Ni (U_{PdCl2} - U_{PdI2} = 30 kJ/mol).[49] This is because Pd is a softer metal, and indeed, PdI_2 is mildly stronger than $PdBr_2$ (U_{PdBr2} - U_{PdI2} = -7 kJ/mol) likely due to the soft-soft interaction between Pd^{2+} and I^-. Still, the difference across the halides is slight, and so lattice energies does support the observation that all Pd salts were reactive enough with didodecyl ditelluride to give palladium telluride. However, the HSAB theory and lattice energies do not explain why $Pd(acac)_2$ gave the palladium-rich phase PdTe; $PdCl_2$ and $PdBr_2$ gave mixtures of PdTe and $PdTe_2$; and PdI_2 yielded only the palladium-poor phase $PdTe_2$. Again, such an observation does not agree with the trends in lattice energies.

Similar to the palladium phases, all the platinum precursors successfully produced $PtTe_2$. The broad XRD peaks (**Figure 2**) indicate small crystallite sizes due to a burst nucleation event. $Pt(acac)_2$ gave the sharpest peaks, suggesting the slowest chemistry of the precursors to yield fewer nuclei growing to larger sizes. In our experiments, $PtCl_2$ left a significant amount of starting material, suggesting it was the least reactive of the halides. Once more, the trend in the size of the crystallites of the produced $PtTe_2$ and unreacted starting material contrasts with HSAB, and while the lattice energies are not reported, HSAB theory predicts that PtI_2 should have the strongest bonds. Experimentally this is, in fact, seen in substitutions of $[Pt(diethylenetriamine)X]^+$ by pyridine, which occur 3.5 times faster for X = Cl^- than for I^-.[55] Like the first-row, HSAB is an insufficient predictor of reactivity for the palladium and platinum halides, and instead the stability of the radical halide is a better predictor of the trends.

Efforts were made to synthesize the ruthenium, palladium, and platinum triflates to further probe the radical stability hypothesis of these second and third-row metals, however, our numerous endeavors were not

successful for the ruthenium and platinum metals using triflic acid or silver triflate. However, a procedure adapted from literature,[47] to synthesize palladium triflate from palladium nitrate and triflic acid was successful; this purple material was prone to decomposition even in air-free conditions. Thus, once palladium triflate was synthesized, it was immediately subjected into the next reaction with didodecyl ditelluride at 135 °C without further purification or characterization. $Pd(OTf)_2$ allowed the formation of $PdTe_2$; in contrast, $PdBr_2$ produced a mixture of mostly PdTe and $PdTe_2$, whereas PdI_2 produced $PdTe_2$. (**Table 1** & **Figure 2**). Since the triflate salt *did* react with the didodecyl ditelluride, two-electron chemistry must be possible on palladium with this reagent. With the enlightening evidence for two-electron chemistry, the reactivity trends of halides further reinforce the statement that HSAB theory is a poor predictor of reactivity and that complex reaction mechanisms are at play. Furthermore, since the palladium triflate solely gave $PdTe_2$, the formation of PdTe must undergo a differing reaction mechanism. Thus, it can be cautiously hypothesized that one-electron chemistry or another complex mechanism explains the formation of PdTe given that palladium has unique metal-carbon chemistry.[56]

Trends were very difficult to identify for the ruthenium precursors. To begin with, the speciation of ruthenium chlorides is often mislabeled and identified. Indeed, the purchased "$RuCl_3$" was found to be $RuOCl_2$ (See Supporting Information). The only product of the reactions with $Ru(acac)_3$ and $RuOCl_2$ was a very small amount of Te(0) and mostly unreacted starting material. Raising the reaction temperatures from 135 °C to 175 °C and 200 °C, saw only more Te(0) form indicating no reaction with the ruthenium salts.

$RuBr_3$ was found to be properly labeled (See Supporting Information), however, interestingly, the product in this case was Ru(0). The only other metal salt in this study to provide M(0) was FeI_2 which was a minor product compared to $FeTe_2$. Control experiments for these two precursors without the tellurium source did not give Ru or Fe metal. A simple redox process is possible, yet an examination of reduction potentials shows that the potential of even Te^{2-} is insufficient to act as a reductant from Ru^{3+} or Fe^{2+} to give their metals ($E°_{Te, Te2-}$ = -1.143 V°, $E°_{Ru3+, Ru2+}$ = 0.2487 V°, $E°_{Ru2+, Ru}$ = 0.455 V°, $E°_{Fe2+, Fe}$ = –0.447 V°).[1] Furthermore, it would be expected that the more noble Pd and Pt would be more likely to be reduced yet were not. $RuBr_3$ will decompose above 400 °C,[57] and perhaps the didodecyl ditelluride may be catalyzing this process. The chemistry of Ru is particularly complicated, and it is possible that both one and two-electron mechanisms are active, especially given that this

metal is also known to perform varied metal-carbon chemistry.[58] In contrast to $RuBr_3$, RuI_3 provided $RuTe_2$ as a product, consistent with the other metal iodides studied. It is unclear why RuI_3 "behaved" while $RuBr_3$ did not, but it is clear that caution and skepticism should be employed when using ruthenium halides as reagents.

It is curious to note that the tellurium-rich phases of all the metals studied, MTe_2 were synthesized almost exclusively, even though MTe are known for many of these metals. Both $FeTe_2$ and $RuTe_2$ contain Te-Te covalent bonds (formally Te_2^{2-} units), whereas the Te-Te bonding is through van der Waals interactions in the layered structures of $CoTe_2$, $NiTe_2$, $PdTe_2$ and $PtTe_2$. Similarly, we achieved the first colloidal synthesis of CuTe (Vulcanite) nanosheets using didodecyl ditelluride, which also features Te-Te van der Waals gaps.[41] It is possible that the proposed one-electron decomposition routes of the didodecyl ditelluride reagent on the metal cations facilitates this type of bonding by selectively breaking the C-Te bonds of the ditellurides. While intermediates from oxidation addition of ditellurides on M(0) complexes have been captured and identified,[59,60,61] we are unaware of any captured intermediates of reactions of ditellurides onto M(II) and M(III) complexes.

Nanocrystal syntheses are most often conducted in the presence of long chain ligands, which not only provide surface capping to growing crystals, but also are increasingly recognized for their ability to moderate the reactivity of the precursors and influence the resultant phases. For this reason, the formation of metal tellurides was repeated in the presence of octadecylamine (**Figure 1**, **Figure 2** & **Table 2)**.

Table 2. Phases (with Octadecylamine)

Precursor	Fe	Co	Ni	Ru[a]	Pd	Pt
$M(acac)_2$	Te	Te	$NiTe_2$, Te	N/A	PdTe	$PtTe_2$
MCl_2	Te	Te	$NiTe_2$	$RuOCl_2$	PdTe	$PtTe_2$
MBr_2	Te	Te	$NiTe_2$	Ru	PdTe, $PdTe_2$	$PtTe_2$
MI_2	$FeTe_2$, Fe, Te	Te	$NiTe_2$	$RuTe_2$	PdTe, $PdTe_2$	$PtTe_2$

[a]All ruthenium precursors utilized were in the +3 oxidation state. The purchased "$RuCl_3$" precursor was analyzed by XRD and found to be $RuOCl_2$.

The comparisons of the reactions with and without octadecylamine highlight the dangers of broadly applying hypothesized mechanisms across metals. For some metals, the presence of the amine does not seem to change product phases (Ru, Pt); in one case the amine enhanced the reactivity with the didodecyl ditelluride and

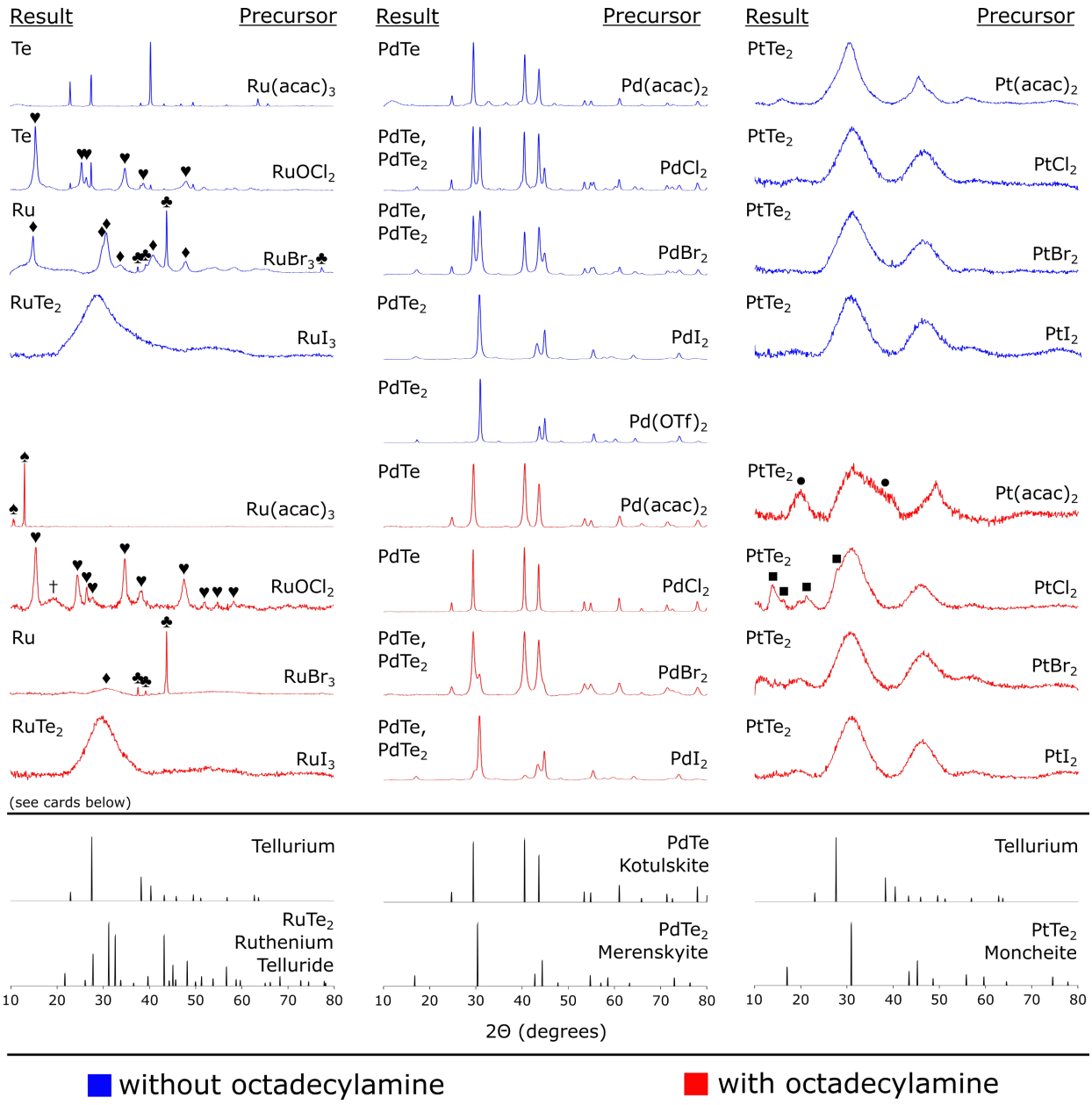

Figure 2. XRD of the products of ruthenium, palladium, and platinum with didodecyl ditelluride. ICDD: ♥ unreacted $RuOCl_2$ - impurity from $RuCl_3$ starting material (See ESI), ♦ $RuBr_3$: #413691, ♣ Ruthenium: #9008513, ♠ $RuC_{17}H_{18}O_3$: #4064886, ● Pt_3O_4: #27836, ■ $PtCl_2$: #28527, Tellurium: #1011098, Ruthenium Telluride: #106001, Kotulskite: #648992, Merenskyite: #648995, Moncheite: #105813.

the formation of metal tellurides (Ni), and in others, decreased the formation of tellurium rich metal tellurides (Fe, Co, Pd).

The addition of octadecylamine to the reaction with FeI_2 introduced a Te(0) impurity. Similarly, the amine with CoI_2 prevents $CoTe_2$ from forming at all. Of peculiar interest, the ligand helps with the formation of $NiTe_2$ for all four metal precursors, not just from $NiBr_2$ and NiI_2.

Is the reason for the unpredictable behavior of the amine that the metals are less reactive, or that the amine speeds the Te decomposition? The situation is complex, but a control experiment indicated that octadecylamine neither inhibited nor sped up the decomposition of didodecyl ditelluride. The amine in most cases should be a stronger ligand than the halides, and ligand substitution may make metal centers more inert or labile, depending on their unique *d* electron counts and coordination geometry. For example Co(II), d^7 amine complexes are likely to have octahedral coordination requiring a dissociative mechanism, and so additional amine would inhibit the reaction with the tellurium precursor. On the other hand Ni(II), d^8 can support four-coordination environments and be open to associative mechanisms. The ligand may provide heightened solubility of the precursor enhancing the reaction with the didodecyl ditelluride. These hypotheses would require detailed mechanistic rate studies to confirm.

If one compares the results of the second and third-row metals with and without octadecylamine the results are similar, however, exceptions are present in this dataset. One exception is that $Ru(acac)_3$ with the ligand provided no crystalline product, and only starting material was recovered. Another is with $RuOCl_2$ where only unreacted starting material is observed, rather than both Te(0) and $RuOCl_2$. Here, the presence of the amine prevented the decomposition of didodecyl ditelluride. The second exception is the trend of the palladium series. The amine appears to improve and promote the formation of PdTe, over $PdTe_2$, possibly by simply slowing down reactivity, or by selectively inhibiting two-electron processes (**Table 1** *vs* **Table 2**) that we identified were needed for the formation of $PdTe_2$ from the $Pd(OTf)_2$ experiment.

No overall trends seem to be present among the transition metals and octadecylamine, and only seem to be metal specific. It is interesting that while the metal precursor is kept constant, different phases are observed with *vs* without the amine. These results are a good starting point especially for $FeTe_2$ and $RuTe_2$, as this is the first colloidal syntheses for these two materials.

The amine also to some extent, influenced size and shape of the products. For $NiTe_2$, the addition of amine caused the formation of defined hexagonal platelets (**Figure 3**) which indicates a strong passivation by amines of the facets perpendicular to the c-direction of the hexagonal $Cd(OH)_2$-type crystal structure. For $RuTe_2$, there was less aggregation of the particles in the presence of amine. In the cannon of nanocrystal synthesis, these

conditions generally did not give highly defined products, however, further lowering of the reaction temperature and reaction optimization may cause a stronger surface passivation, which might lead to more defined faceting and size control for the other metal tellurides beyond $NiTe_2$.

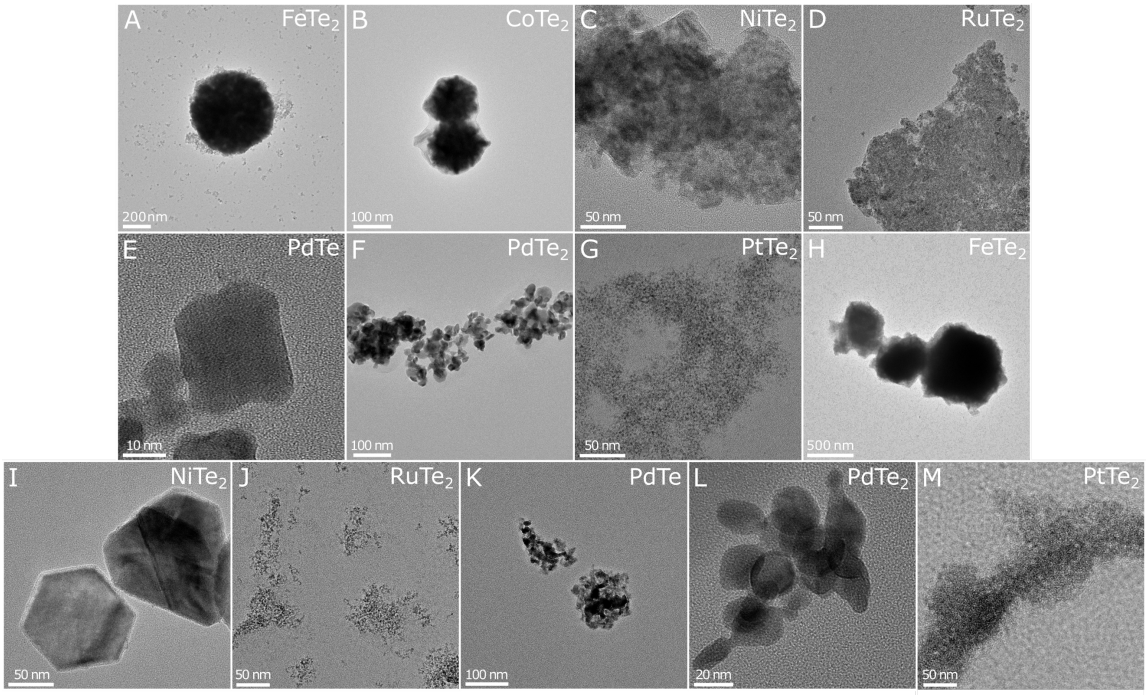

Figure 3. Representative TEM images of iron, cobalt, nickel, ruthenium, palladium, and platinum tellurides. A variety of metal precursors (see above) were reacted with didodecyl ditelluride either with or without the presence of octadecylamine at a mild temperature of 135 °C for 1h. **A-G:** Representative TEM images without octadecylamine **A.** from FeI_2, **B.** from CoI_2, **C.** from NiI_2, **D.** from RuI_3, **E.** $Pd(acac)_2$, **F.** from PdI_2, **G.** from $PtCl_2$. **H-M:** Representative TEM images with octadecylamine **H.** from FeI_2, **I.** from NiI_2, **J.** from RuI_3, **K.** from $Pd(acac)_2$, **L.** from PdI_2, **M.** from $PtBr_2$.

Conclusion

Didodecyl ditelluride was used as a reagent in the synthesis of transition metal tellurides at a moderate temperature of 135 °C. $FeTe_2$ (Frohbergite), $CoTe_2$ (Cobalt Telluride), $NiTe_2$ (Melonite), $RuTe_2$ (Ruthenium Telluride), PdTe (Kotulskite), $PdTe_2$ (Merenskyite) and $PtTe_2$ (Moncheite) were synthesized. These represent the first colloidal syntheses to $FeTe_2$ (Frohbergite) and $RuTe_2$ (Ruthenium Telluride). The seeming tendency to form MTe_2 phases rather than MTe phases in many of the reactions suggests that possibly the mechanism involves selective breaking of C-Te bonds in didodecyl ditelluride over Te-Te bonds. Through an extensive and systematic study of MX_2 (and RuX_3) precursors, it was found that the choice of the coordinating anion, X^-, was instrumental

to the success of the reaction. Chosen metal precursors included the acetylacetonates, chlorides, bromides, iodides, and triflates of the six aforementioned-transition metals.

Among the first-row transition-metal salts of Fe, Co, and Ni, only the iodides consistently gave metal telluride phases, while others only provided tellurium metal. Initially, HSAB theory and known lattice energies of the halide precursors were used to explain some of the outcomes, but application of these hypotheses failed to fully explain the trends observed. Instead, mechanistic insight from the comparison of the resulting phases of first-row transition metal triflates *vs* halides suggested that the formation of MTe_2 undergoes a one-electron mechanistic route. Thus, radical stability was instead found to be the better predictor of MX_2 reactivity over HSAB. Additionally, attempts were made to synthesize metal triflates of the second and third-row metals, but only $Pd(OTf)_2$ was successful. Reactions with this triflate reagent suggest, in comparison to the halides, that a two-electron mechanism furnishes $PdTe_2$, whereas a one-electron route yields PdTe.

The addition of octadecylamine as a ligand did not provide consistent reaction patterns across the metals studied. Sometimes it promoted the production of the metal telluride, and in others it was a hindrance. While we attempted to identify and interpret trends across the late transition metals, the study with added amine gives us pause; each metal with its unique electron configuration may require individual consideration outside of its neighbors on the periodic table.

This work is just the tip of the iceberg of what the nanomaterial community truly needs to be able to predictably understand how phases form. These types of systematic studies will provide the basis for rational approaches to the syntheses of more complex phases and, by extension, sophisticated technological applications of those materials that we are currently unable to access or foresee with our present toolset. Mechanistic understanding of *how* phases form will become essential in the future to rationally synthesize materials for more elaborate applications.

Author Information

Corresponding Author
⸸ J. E. Macdonald. Email: janet.macdonald@vanderbilt.edu

ORCID
Danielle N. Penk: 0000-0001-5575-5847
Emma J. Endres: 0000-0001-7951-3623
Ahmed Y. Nuriye: 0000-0002-8210-000X
Janet E. Macdonald: 0000-0001-6256-0706

Notes
The authors declare no competing financial interest.

Works Cited

(1) Electrochemical Series. In *CRC Handbook of Chemistry and Physics*; Lide, D., Frederikse, H., Eds.; CRC Press, Inc., 1994; pp 8.21-8.31.

(2) Vivanco, H.; Rodriguez, E. The Intercalation Chemistry of Layered Iron Chalcogenide Superconductors. *J. Solid State Chem.* **2016**, *242*, 3–21.

(3) Liu, Z.; Li, Z.; Xie, X.; Yang, S.; Fei, J.; Li, Y.; Xu, Z.; Liu, H. Development of Recyclable Iron Sulfide/Selenide Microparticles with High Performance for Elemental Mercury Capture from Smelting Flue Gas over a Wide Temperature Range. *Environ. Sci. Technol.* **2020**, *54*, 604–612.

(4) Maneeprakorn, W.; Malik, M.; O'Brien, P. The Preparation of Cobalt Phosphide and Cobalt Chalcogenide (CoX, X = S, Se) Nanoparticles from Single Source Precursors. *J. Mater. Chem.* **2010**, *20*, 2329–2335.

(5) Butterfield, A.; McCormick, C.; Veglak, J.; Schaak, R. Morphology-Dependent Phase Selectivity of Cobalt Sulfide during Nanoparticle Cation Exchange Reactions. *J. Am. Chem. Soc.* **2021**, *143*, 7915–7919.

(6) Ren, H.; Huang, Z.; Yang, Z.; Tang, S.; Kang, F.; Lv, R. Facile Synthesis of Free-Standing Nickel Chalcogenide Electrodes for Overall Water Splitting. *J. Energy Chem.* **2017**, *26*, 1217–1222.

(7) Li, C.; Li, X. Yang, S.; Wang, H.; Wang, G. Synthesis of Controllable Nickel Chalcogenide Nano-Hollow Spheres and Their Tunable Absorbing Properties. *ChemistrySelect* **2020**, *5*, 8185–8193.

(8) Mbese, J.; Ajibade, P. Homonuclear Tris-Dithiocarbamato Ruthenium(III) Complexes as Single-Molecule Precursors for the Synthesis of Ruthenium(III) Sulfide Nanoparticles. *J. Sulfur Chem.* **2016**, *38*, 173–187.

(9) Zhao, Y.; Cong, H.; Li, P.; Wu, D.; Chen, S.; Luo, W. Hexagonal RuSe2 Nanosheets for Highly Efficient Hydrogen Evolution Electrocatalysis. *Angew. Chem. Int. Ed.* **2021**, *60*, 7013–7017.

(10) Kumar, A.; Rao, G.; Kumar, S.; Singh, A. Formation and Role of Palladium Chalcogenide and Other Species in Suzuki-Miyaura and Heck C-C Coupling Reactions Catalyzed with Palladium(II) Complexes of Organochalcogen Ligands: Realities and Speculations. *Organometallics* **2014**, *33*, 2921–2943.

(11) Musetha, P.; Revaprasadu, N.; Kolawole, G.; Pullabhotla, R.; Ramasamy, K.; O'Brien, P. Homoleptic Single Molecular Precursors for the Deposition of Platinum and Palladium Chalcogenide Thin Films. *Thin Solid Films* **2010**, *519*, 197–202.

(12) Li, Z.; Zeng, Y.; Zhou, M.; Xie, B.; Zhang, J.; Wu, W. Suppression of Magnetoresistance in PtSe2 Microflakes with Antidot Arrays. *Nanotechnology* **2018**, *29*, 40LT01.

(13) Arora, A.; Oswal, P.; Datta, A.; Kumar, A. Complexes of Metals with Organotellurium Compounds and Nanosized Metal Tellurides for Catalysis, Electrocatalysis and Photocatalysis. *Coord. Chem. Rev.* **2022**, *459*, 214406.

(14) Park, G.; Kang, Y. Conversion Reaction Mechanism for Yolk-Shell-Structured Iron Telluride-C Nanospheres and Exploration of Their Electrochemical Performance as an Anode Material for Potassium-Ion Batteries. *Small Methods* **2020**, *4*, 2000556.

(15) Pradhan, S.; Pramanik, S.; Das, D.; Bhar, R.; Bandyopadhyay, R.; Millner, P.; Pramanik, P. Nanosized Iron Telluride for Simultaneous Nanomolar Voltammetric Determination of Dopamine, Uric Acid, Guanine and Adenine. *New J. Chem.* **2019**, *43*, 10590–10600.

(16) Gao, Q.; Huang, C.; Ju, Y.; Gao, M.; Liu, J.; An, D.; Cui, C.; Zheng, Y.; Li, W.; Yu, S. Phase-Selective Syntheses of Cobalt Telluride Nanofleeces for Efficient Oxygen Evolution Catalysts. *Angew. Chem. Int. Ed.* **2017**, *56*, 7769–7773.

(17) Patil, S.; Kim, E.; Shrestha, N.; Chang, J.; Lee, J.; Han, S. Formation of Semimetallic Cobalt Telluride Nanotube Film via Anion Exchange Tellurization Strategy in Aqueous Solution for Electrocatalytic Applications. *ACS Appl. Mater. Interfaces* **2015**, *7*, 25914–25922.

(18) Khan, M.; Ashiq, M.; Ehsan, M.; He, T.; Ijaz, S. Controlled Synthesis of Cobalt Telluride Superstructures for the Visible Light Photo-Conversion of Carbon Dioxide into Methane. *Appl. Catal. A: Gen.* **2014**, *487*, 202–209.

(19) Silva, U.; Masud, J.; Zhang, N.; Hong, Y.; Liyanage, W.; Zaeem, M.; Nath, M. Nickel Telluride as a Bifunctional Electrocatalyst for Efficient Water Splitting in Alkaline Medium. *J. Mater. Chem. A* **2018**, *6*, 7608–7622.

(20) Zhao, B.; Dang, W.; Liu, Y.; Li, B.; Li, J.; Luo, J.; Zhang, Z.; Wu, R.; Ma, H.; Sun, G.; Huang, Y.; Duan, X.; Duan, X. Synthetic Control of Two-Dimensional NiTe2 Single Crystals with Highly Uniform Thickness Distributions. *J. Am. Chem. Soc.* **2018**, *140*, 14217–14223.

(21) Chia, X.; Sofer, Z.; Luxa, J.; Pumera, M. Unconventionally Layered CoTe2 and NiTe2 as Electrocatalysts for Hydrogen Evolution. *Chem. Eur. J.* **2017**, *23*, 11719–11726.

(22) Sharma, K.; Joshi, H.; Sharma, A.; Prakash, O.; Singh, A. Single Source Precursor Routes for Synthesis of PdTe Nanorods and Particles: Solvent Dependent Control of Shapes. *Chem. Commun.* **2013**, *49*, 9344–9346.

(23) Arora, A.; Oswal, P.; Rao, G.; Kumar, S.; Singh, A.; Kumar, A. Catalytically Active Nanosized Pd9Te4 (Telluropalladinite) and PdTe (Kotulskite) Alloys: First Precursor-Architecture Controlled Synthesis Using Palladium Complexes of Organotellurium Compounds as Single Source Precursors. *RSC Adv* **2021**, *11*, 7214–7224.

(24) Arora, A.; Oswal, P.; Rao, G.; Kumar, S.; Singh, A.; Kumar, A. Tellurium-Ligated Pd(II) Complex of Bulky Organotellurium Ligand as a Catalyst of Suzuki Coupling: First Report on In Situ Generation of Bimetallic Alloy 'Telluropalladinite' (Pd9Te4) Nanoparticles and Role in Highly Efficient Catalysis. *Catal. Letters* **2022**, *152*, 1999–2011.

(25) Fu, L.; Hu, D.; Mendes, R.; Rümmeli, M.; Dai, Q.; Wu, B.; Fu, L.; Liu, Y. Highly Organized Epitaxy of Dirac Semimetallic PtTe2 Crystals with Extrahigh Conductivity and Visible Surface Plasmons at Edges. *ACS Nano* **2018**, *12*, 9405–9411.

(26) Supriya, S.; Antonatos, N.; Luxa, J.; Gusmão, R.; Sofer, Z. Comparison between Layered Pt3Te4 and PtTe2 for Electrocatalytic Reduction Reactions. *FlatChem* **2021**, *29*, 100280.

(27) Oyetunde, T.; Afzaal, M.; O'Brien, P. Phenyl Substituted Ditelluro-Imidodiphosphinate Complexes of Iron, Nickel, Palladium, Platinum, and Their Pyrolysis Studies Generating Metal Tellurides. *Polyhedron* **2019**, *160*, 157–162.

(28) de Los Reyes, J. Ruthenium Sulfide Supported on Alumina as Hydrotreating Catalyst. *Appl. Catal. A: Gen.* **2007**, *322*, 106–112.

(29) Krishnamoorthy, K.; Pazhamalai, P.; Kim, S. Ruthenium Sulfide Nanoparticles as a New Pseudocapacitive Material for Supercapacitor. *Electrochim. Acta* **2017**, *227*, 85–94.

(30) Gu, X.; Yang, X. Feng, L. An Efficient RuTe2/Graphene Catalyst for Electrochemical Hydrogen Evolution Reaction in Acid Electrolyte. *Chem. Asian J.* **2020**, *15*, 2886–2891.

(31) Tsay, M.; Huang, J.; Chen, C.; Huang, Y. Crystal Growth in Tellurium Flux and Characterization of Ruthenium Dichalcogenides. *Mater. Res. Bull.* **1995**, *30*, 85–92.

(32) *Binary Alloy Phase Diagrams*, 2nd ed.; Massalski, T., Okamoto, H., Subramanian, P., Kacprzak, L., Eds.; ASM International, 1990; Vol. 2.

(33) *Binary Alloy Phase Diagrams*, 2nd ed.; Massalski, T., Okamoto, H., Subramanian, P., Kacprzak, L., Eds.; ASM International, 1990; Vol. 3.

(34) Jiang, L.; Yuan, R.; Chai, Y.; Yuan, Y.; Bai, L.; Wang, Y. An Ultrasensitive Electrochemical Aptasensor for Thrombin Based on the Triplex-Amplification of Hemin/G-Quadruplex Horseradish Peroxidase-Mimicking DNAzyme and Horseradish Peroxidase Decorated FeTe Nanorods. *Analyst* **2013**, *138*, 1497–1503.

(35) Pradhan, S.; Das, R.; Biswas, S.; Das, D.; Bhar, R.; Bandyopadhyay, R.; Pramanik, P. Chemical Synthesis of Nanoparticles of Nickel Telluride and Cobalt Telluride and Its Electrochemical Applications for Determination of Uric Acid and Adenine. *Electrochim Acta* **2017**, *238*, 185–193.

(36) Masikini, M.; Ndangili, P.; Ikpo, C.; Feleni, U.; Duoman, S.; Sidwaba, U.; Waryo, T.; Baker, P.; Iwuoha, E. Optoelectronics of Stochiometrically Controlled Palladium Telluride Quantum Dots. *J. Nano Res.* **2016**, *40*, 29–45.

(37) Ulbrich, K.; Bertolotti, F.; Masciocchi, N.; Cervellino, A.; Guagliardi, A.; Campos, C. A Comprehensive Structural and Microstructural Investigation of a New Iron-Telluride Nano Phase. *J. Mater. Chem. C* **2018**, *6*, 3047–3057.

(38) Yuan, M.; Li, Q.; Zhang, J.; Wu, J.; Zhao, T.; Liu, Z.; Zhou, L.; He, H.; Li, B.; Zhang, G. Engineering Surface Atomic Architecture of NiTe Nanocrystals Toward Efficient Electrochemical N2 Fixation. *Adv. Funct. Mater.* **2020**, *30*, 2004208.

(39) Xie, Yi.; Li, B.; Su, H.; Liu, X.; Qian, Y. Solvothermal Route to CoTe2 Nanorods. *Nanostructured Materials* **1999**, *11*, 539–544.

(40) Fenton, J.; Fagan, A.; Schaak, R. General Solution-Phase Synthesis of Nanoscale Transition Metal Tellurides Using Metal Nanoparticle Reagents. *Eur. J. Inorg. Chem.* **2019**, 3490–3493.

(41) Robinson, E.; Dwyer, K.; Koziel, A.; Nuriye, A.; Macdonald, J. Synthesis of Vulcanite (CuTe) and Metastable Cu1.5Te Nanocrystals Using a Dialkyl Ditelluride Precursor. *Nanoscale* **2020**, *12*, 23036–23041.

(42) Peng, Z.; Peng, X. Formation of High-Quality CdTe, CdSe, and CdS Nanocrystals Using CdO as Precursor. *J. Am. Chem. Soc.* **2001**, *123*, 183–184.

(43) Anderson, N.; Hendricks, M.; Choi, J.; Owen, J. Ligand Exchange and the Stoichiometry of Metal Chalcogenide Nanocrystals: Spectroscopic Observation of Facile Metal-Carboxylate Displacement and Binding. *J. Am. Chem. Soc.* **2013**, *135*, 18536–18548.

(44) Drijvers, E.; de Roo, J.; Martins, J.; Infante, I.; Hens, Z. Ligand Displacement Exposes Binding Site Heterogeneity on CdSe Nanocrystal Surfaces. *Chem. Mater.* **2018**, *30*, 1178–1186.

(45) Nag, A.; Zhang, H.; Janke, E.; Talapin, D. Inorganic Surface Ligands for Colloidal Nanomaterials. *Z. Phys. Chem.* **2015**, *229*, 85–107.

(46) Sales, B. Chapter 1: Introduction to the Synthesis of Quantum Materials: Some General Guidelines and A Few Tricks. In *Fundamentals of Quantum Materials: A Practical Guide to Synthesis and Exploration*; 2021; pp 1–17.

(47) Murata, S.; Ido, Y. Practical Synthesis of Palladium Bis(Trifluoromethanesulfonate) and Its Application to the Synthesis of Palladium Complexes. *Bull. Chem. Soc. Jpn.* **1994**, *67*, 1746–1748.

(48) Hernández-Pagán, E.; Robinson, E.; la Croix, A.; Macdonald, J. Direct Synthesis of Novel Cu2-XSe Wurtzite Phase. *Chem. Mater.* **2019**, *31*, 4619–4624.

(49) Lattice Energies. In *CRC Handbook of Chemistry and Physics*; Rumble, J. R., Ed.; CRC Press/Taylor & Francis: Boca Raton, FL, 2021.

(50) Smith, M.; March, J. *March's Advanced Organic Chemistry: Reactions, Mechanisms, and Structure*, 5th ed.; John Wiley & Sons, Inc., 2001.

(51) Kürti, L.; Czakó, B. *Strategic Applications of Named Reactions in Organic Synthesis*; Elsevier Inc., 2005.

(52) Smith, W.; Branum, G. The Abnormal Finkelstein Reaction. A Sequential Ionic-Free Radical Reaction Mechanism. *Tetrahedron Lett* **1981**, *22*, 2055–2058.

(53) Smith, M.; March, J. *March's Advanced Organic Chemistry: Reactions, Mechanisms, and Structure*, 5th ed.; John Wiley & Sons, Inc., 2001.

(54) Kobayashi, S.; Sugiura, M.; Kitagawa, H.; Lam, W. Rare-Earth Metal Triflates in Organic Synthesis. *Chem. Rev.* **2002**, *102*, 2227–2302.

(55) Basolo, F.; Gray, H.; Pearson, R. Mechanism of Substitution Reactions of Complex Ions. XVII. Rates of Reaction of Some Platinum(II) and Palladium(II) Complexes with Pyridine. *J. Am. Chem. Soc.* **1960**, *82*, 4200–4203.

(56) Lee, S.; Lee, W.; Sulikowski, G. An Enantioselective 1,2-Aziridinomitosene Synthesis via a Chemoselective Carbon-Hydrogen Insertion Reaction of a Metal Carbene. *J. Org. Chem.* **1999**, *64*, 4224–4225.

(57) Greenwood, N.; Earnshaw, A. Halides and Oxohalides. In *Chemistry of the Elements*; Reed Educational and Professional Publishing Ltd: Great Britain, 1997; pp 1082–1083.

(58) Xu, Y.; Wong, J.; Samkian, A.; Ko, J.; Chen, S.; Houk, K.; Grubbs, R. Efficient Z-Selective Olefin-Acrylamide Cross-Metathesis Enabled by Sterically Demanding Cyclometalated Ruthenium Catalysts. *J. Am. Chem. Soc.* **2020**, *142*, 20987–20993.

(59) Jain, V.; Chauhan, R. New Vistas in the Chemistry of Platinum Group Metals with Tellurium Ligands. *Coord. Chem. Rev.* **2016**, *306*, 270–301.

(60) Karjalainen, M.; Wiegand, T.; Rautiainen, J.; Wagner, A.; Görls, H.; Weigand, W.; Oilunkaniemi, R.; Laitinen, R. Competitive Te-Te and C-Te Bond Cleavage in the Oxidative Addition of Diaryl and Dialkyl Ditellurides to Pt(0) Centers. *J. Organomet. Chem.* **2017**, *836–837*, 17–25.

(61) Polo, A.; Real, J. 39.32.2.1 Synthesis of Product Subclass 2. In *Science of Synthesis*; 2008; Vol. 39, pp 1145–1161.